Journal of Solid State Chemistry **163,** 84–92 (2002)
doi:10.1006/jssc.2001.9376, available online at http://www.idealibrary.com on IDEAL®

Structure and Thermal Stability of $La_{0.10}WO_{3+y}$; A Hexagonal Tungsten Bronze Related Phase Formed at High Pressure

V. P. Filonenko,* C. Grenthe,† M. Nygren,† M. Sundberg,†,[1] and I. P. Zibrov‡

*Institute for High Pressure Physics, Russian Academy of Sciences, Troitsk, 142190, Moscow Region, Russia; †Department of Inorganic Chemistry, Arrhenius Laboratory, Stockholm University, SE-106 91 Stockholm, Sweden; and ‡Institute of Crystallography, Russian Academy of Sciences, 117333 Moscow, Russia

Received May 30, 2001; in revised form August 16, 2001; accepted August 23, 2001

The structure and thermal stability of a hexagonal tungsten bronze (HTB) related compound, La_xWO_{3+y} with $x \approx 0.10$ and $y \approx 0.15$, has been studied by X-ray diffraction, thermal analysis, and electron microscopy. The structure was refined by the Rietveld method from X-ray powder diffractometer data of a $La_{0.10}WO_3$ sample prepared at $T = 1250°C$ and $P = 25$ kbar, which consisted of two tungsten bronze related phases in 1:1 proportion. The unit cell dimensions are as follows: $La_{0.108}WO_{3+y}$ ($y \approx 0.16$), $a = 7.40890(5)$, and $c = 3.79239(4)$ Å (HTB-related structure); $La_{0.091}WO_3$, $a = 3.82458(6)$ Å (cubic perovskite tungsten bronze (PTB) structure). The lanthanum atoms in $La_{0.108}WO_{3+y}$ are located on the hexagonal axis and statistically distributed on two sites close to the tungsten atom plane. Thermal stability studies of the $La_{0.10}WO_3$ sample in an argon atmosphere under ambient pressure conditions revealed that the HTB-related compound is metastable, decomposing to the stable PTB-type structure and WO_3. It was also found from the TG experiments in argon and oxygen that additional oxygen atoms (y) are present in the structure, thus forming a lanthanum tungsten oxide of the above composition. The electron diffraction and microanalysis studies confirmed that crystals of the HTB- and PTB-type structures were formed, with a lanthanum content of $x \approx 0.1$. © 2002 Elsevier Science

INTRODUCTION

Hexagonal tungsten bronze (HTB) related phases of the general formula RE_xWO_3 have recently been found in multiphase lanthanum– and neodymium–tungsten oxide samples prepared by solid-state reaction under high-pressure and high-temperature conditions (1, 2). From microanalysis studies of individual HTB crystallites in the transmission electron microscope, the x value was determined to be $x \approx 0.1$. Previous X-ray diffraction studies of $RE_{0.1}WO_3$ samples prepared by conventional high-temperature solid-state synthesis have shown that perovskite tungsten bronze (PTB) phases are formed (3, 4).

The crystal structure of the hexagonal tungsten bronze M_xWO_3 can be described as a network of corner-sharing WO_6 octahedra arranged so that three- and six-sided tunnels are created along the hexagonal axis (5), as shown in Fig. 1. The M atoms enter interstitial sites in the six-sided tunnels, and when these sites are fully occupied, the value of x is 0.33. HTB-type tungsten bronzes of the heavier alkali metals (K, Rb, and Cs) and of some electropositive elements like In, Tl, and Ge (6–8) are known to form by solid-state reaction under ambient pressure conditions. Several X-ray structure determinations have been reported concerning the off-center displacement of the tungsten atoms in the octahedra and the location and occupancy of the M atom sites in the six-sided tunnels (7–10).

HTB-related phases have also been prepared by soft chemistry methods. Gerand *et al.* (11) have synthesized a hexagonal modification of WO_3, which is isostructural with HTB except that the tunnel sites are empty. The hexagonal form is metastable and transforms irreversibly to the monoclinic modification of WO_3 at about 400°C (12). The hexagonal WO_3 structure can be stabilized, however, by insertion of other elements such as Li, Na, and Mg through an intercalation reaction, and the corresponding HTB bronzes have been thus prepared (13–15). It should also be mentioned that a hexagonal tin tungsten bronze, Sn_xWO_3 ($x = 0.26 - 0.33$), has recently been prepared under mild reaction conditions, and its crystal structure has been determined from single-crystal X-ray data (16).

The structural studies of the HTB bronzes have shown that the larger cations (K^+, Rb^+, Cs^+, Tl^+, and In^+) occupy positions in the hexagonal tunnels between the tungsten layers (5, 7, 9, 10). The tungsten atoms in a layer are also displaced in the xy plane from the center of the octahedra with respect to the ones above and below, thus forming a puckered structure with a corresponding doubling of the

[1] To whom correspondence should be addressed. Fax: +468152187. E-mail: marsu@inorg.su.se.

0022-4596/02 $35.00

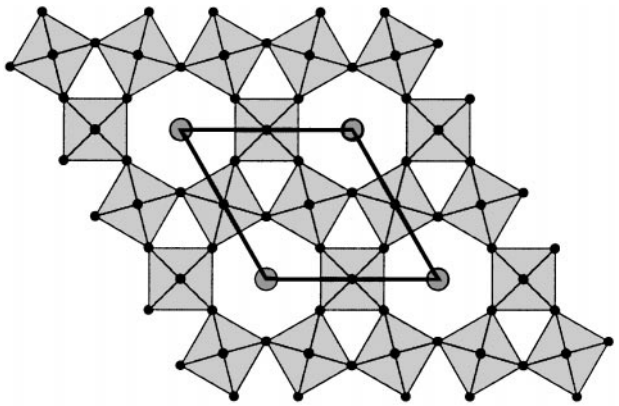

FIG. 1. Structure model of the hexagonal tungsten bronze (HTB) M_xWO_3, viewed along the c axis. The M atoms are represented as dark spots and the unit cell is outlined. The representation of the structure was produced with ATOMS by Shape Software.

c axis. The smaller cations, Ge^{2+} (8) and Sn^{2+} (16), on the other hand, are located in the hexagonal tunnels in the same plane as the tungsten atoms. The tungsten atoms are located here at the center of the octahedra, thus forming a more regular HTB structure with a c axis of ≈ 3.8 Å. The present study was undertaken to investigate the structure and phase stability of the HTB-related phase $La_{0.1}WO_3$, formed under high-pressure and high-temperature conditions, by a combination of X-ray powder diffraction, thermal analysis, and electron microscopy methods.

EXPERIMENTAL

The starting materials were La_2O_3, WO_3, and W-metal powder, all of high-purity grade. Weighed mixtures of $La_{0.10}WO_3$ composition were carefully ground in an agate mortar, both as dry powders and under acetone. The resulting dry mixtures were pressed to pellets, which were then covered by tungsten foil to avoid chemical reaction with the surrounding high-pressure cell material. The syntheses were performed using the high-pressure equipment and method recently described in Ref. (17). One sample (denoted *hp*1) was prepared at $T = 1250$°C and $P = 25$ kbar, whereas the other two preparations, *hp*2 and *hp*3, were made at $T = 1200$°C and $P = 50$ and 80 kbar, respectively (Table 4). One sample of composition $La_{0.10}WO_3$ was also prepared under ambient pressure (*ap*) by the conventional high-temperature solid-state method. The starting mixture was thus annealed in an evacuated silica tube at $T = 900$°C for 3 days (Table 4). The resulting powder was re-ground and heated again in an evacuated silica tube at 900°C for another 3 days. This sample (denoted *ap*) was used as reference material in the thermal analysis studies.

X-ray powder photographs were taken in a subtraction-geometry Guinier–Hägg focusing camera, with strictly monochromatized Cu$K\alpha_1$ radiation. Si was used as an internal standard. The photographs were evaluated in an automatic film scanner system (18), and the unit cell parameters were refined from the X-ray data with the PIRUM program (19). A HUBER Imaging Plate Guinier camera was also used in the phase analysis studies.

The electron microscopy specimens were prepared in the following way: a small amount of the sample was crushed in an agate mortar and dispersed in *n*-butanol. A few drops of the suspension were collected on a perforated carbon film supported on a Cu grid. The electron microscopy investigations were then carried out with a scanning electron microscope JEOL 820 (SEM) and a transmission electron microscope JEOL 2000FXII (TEM). Both microscopes were equipped with LINK AN10000 EDS microanalysis systems. The microanalysis results are based on the La*L* and W*L* lines in the EDS spectra. Combined electron diffraction and microanalysis studies of individual crystal fragments were made in the TEM microscope.

The thermal stability of the obtained products was studied by simultaneous recordings of the thermogravimetric (TG) and differential thermal analysis (DTA) curves (Fig. 3) and by thermogravimetric analysis (Fig. 5) using a Setaram TAG24 instrument. The error in the thermogravimetric measurement in the combined TG/DTA study is estimated to be ± 0.03 wt%, and the corresponding values for the data presented in Figs. 5 and 6 are ± 0.01 and ± 0.05 wt%, respectively. The samples were heated in Al_2O_3 cups, and measurements were performed in an argon atmosphere, from room temperature to 850°C, at a heating rate of 10°C min^{-1}. The oxidation studies were carried out in an oxygen atmosphere in a Perkin–Elmer TGA7 instrument. The samples were heated in Pt cups at a rate of 3°C min^{-1} from room temperature to 850°C.

X-RAY DIFFRACTION STUDIES

The Guinier powder patterns taken of the three high-pressure samples *hp*1–*hp*3 displayed strong peaks characteristic of an HTB phase with unit cell dimensions of $a \approx 7.40$ Å and $c \approx 3.79$ Å. No single-phase sample was formed. The X-ray data showed that the sample prepared at 25 kbar (*hp*1) contained a mixture of two tungsten bronze related phases in $\sim 1:1$ proportion; one was of PTB type and the other of HTB type. The refined unit cell parameters are given in Table 1. According to the X-ray patterns, the samples prepared at 50 kbar (*hp*2) and 80 kbar (*hp*3) consisted of approximately 90 wt% of the HTB-related compound. A small amount of WO_3 seemed also to be present in *hp*2, whereas *hp*3, prepared at the highest pressure, contained some of the high-pressure oxide, W_3O_8(II) (20). The X-ray powder pattern of $La_{0.10}WO_3$ (*ap* sample) showed lines characteristic of a perovskite tungsten bronze (PTB) with cubic symmetry ($a = 3.840$ Å).

TABLE 1
Experimental Details for the $La_{0.10}WO_3$ Sample, *hp*1, Prepared at 25 kbar

Chemical formula	$La_{0.091}WO_3$	$La_{0.108}WO_3$	$La_{0.108}WO_{3+y}$
Space group	*Pm*3*m*	*P*6/*mmm*	
Z	1	3	
F.W. (at 298 K)	244.488	740.548	
a (Å)	3.82458(6)	7.40890(5)	
c (Å)		3.79239(4)	
V (Å^3)	55.9435(15)	180.2818(24)	
d-calc. (g/cm^3)	7.257	6.821	(6.893)
Weight fraction	0.477(2)	0.523(2)	
R_F	0.0284	0.0647	(0.0612)
R_P	0.0819	0.0819	(0.0796)
R_{WP}	0.1104	0.1104	(0.1068)
d	0.507	0.507	(0.537)
$FWHM_{min}$ (°)	0.108	0.119	
$FWHM_{max}$ (°)	0.562	0.191	
No. of parameters used	38	38	(39)

Note. *d* = Durbin–Watson statistic *d*-value according to Hill and Flack (23).

Electron diffraction (ED) patterns taken in different orientations of the HTB crystallites did not show any superstructure reflections characteristic of a doubled *c* axis. The ED results thus confirmed the unit cell parameters given in Table 1 and supported the planar space group *P*6/*mmm* used in the X-ray refinement of the HTB structure described below. The *c*-axis length (3.79 Å) indicated that the HTB structure of La_xWO_3 is closely related to those of Sn_xWO_3 (16) and $Ge_{0.24}WO_3$ (8). The sample *hp*1 was chosen for further structural studies by the Rietveld method.

X-ray powder diffraction data for the structure refinement of the sample *hp*1 were collected on a Stoe Stadi/P diffractometer with a rotating sample in symmetric transmission mode. A symmetric focusing germanium monochromator (focal distance = 440 mm) was used to give pure Cu$K\alpha_1$ radiation ($\lambda = 1.540598$ Å). The diffraction data were collected with a small linear-position-sensitive detector (PSD) covering 6.4° in 2θ. The PSD was moved in steps of 0.2°, 300 s/step, thus giving an average intensity of 32 measurements at each 2θ position. It has been found that the angular resolution of the diffractometer operated under these conditions is approximately the same as that of a Guinier–Hägg photograph. The 2θ range measured was $10° < 2\theta < 130°$. The software program package GSAS (21) was used for the Rietveld refinement. The peak shapes were described by a symmetric pseudo-Voigt function. The atoms in the PTB structure were placed at the special sites of the ideal cubic unit cell as in $La_{0.14}WO_3$ (4). The positions of the W and O atoms in the HTB structure were taken from the structure determination of $Ge_{0.24}WO_3$ (8) and were held fixed during the refinement. Structural refinements of three

TABLE 2
Fractional Atomic Coordinates and Equivalent Isotropic Displacement Parameters (Å^2) for $La_{0.091}WO_3$ (PTB-Type Structure) ($U_{eq} = (\frac{1}{3})\sum_i\sum_j U^{ij}a^ia^ja_ia_j$)

Atom	Site	OCC	*x*	*y*	*z*	U_{eq}
La	(1*a*)	0.091(4)	0	0	0	0.0022(27)
W	(1*b*)	1.000	½	½	½	0.0137(4)
O1	(3*c*)	1.000	0	½	½	0.0132(20)

HTB models have been performed. In the first model, the La atom was located at the (*x*, *y*, 0) position, which is analogous to Sn in Sn_xWO_3 (16). In the second one, the La atom was placed at (*x*, 0, 0), which is isotypic with Ge in $Ge_{0.24}WO_3$ (8); and in the last model, the La atom was displaced out of the *xy* plane and located at the (0, 0, *z*) position. The latter model seemed to be the most reasonable one, as the Rietveld refinements of the first two models did not converge. However, the occupancy of the La position (0, 0, *z*) in the HTB structure could not be obtained from the refinement due to strong correlation with the isotropic displacement parameters. On the other hand, the occupancy of the La site in the PTB structure and the weight fractions of the PTB and the HTB phases in the bulk sample could be refined. From these two parameters and from the La content in the starting material ($x = 0.10$), the occupancy of the La position in the HTB structure could be estimated to be $x = 0.108$; this value was held fixed during further refinement. This decreased the e.s.d's and R ($R_f = 0.0647$). The crystal data and data from the final Rietveld refinement are given in Table 1. The atom parameters for the PTB and HTB structures are given in Tables 2 and 3, respectively. The thermal parameters given in the latter two tables should be regarded with caution because absorption phenomena are not taken into account. The observed, calculated, and difference profiles are shown in Fig. 2.

TABLE 3
Fractional Atomic Coordinates and Equivalent Isotropic Displacement Parameters (Å^2) for $La_{0.108}WO_{3+y}$ (HTB Related Structure); The Coordinates of the Additional Oxygen Atom ($y = 0.162$) Is Given Within Parentheses ($U_{eq} = (\frac{1}{3})\sum_i\sum_j U^{ij}a^ia^ja_ia_j$)

Atom	Site	OCC	*x*	*y*	*z*	U_{eq}
La	(2*e*)	0.162	0	0	0.048(4)	0.0087(31)
W	(3*f*)	1.000	0	½	0	0.0050(4)
O1	(3*g*)	1.000	½	0	½	− 0.0106(23)
O2	(6*l*)	1.000	0.208	0.416	0	0.0112(31)
(O3	(1*b*)	0.486	0	0	½	0.042(19))

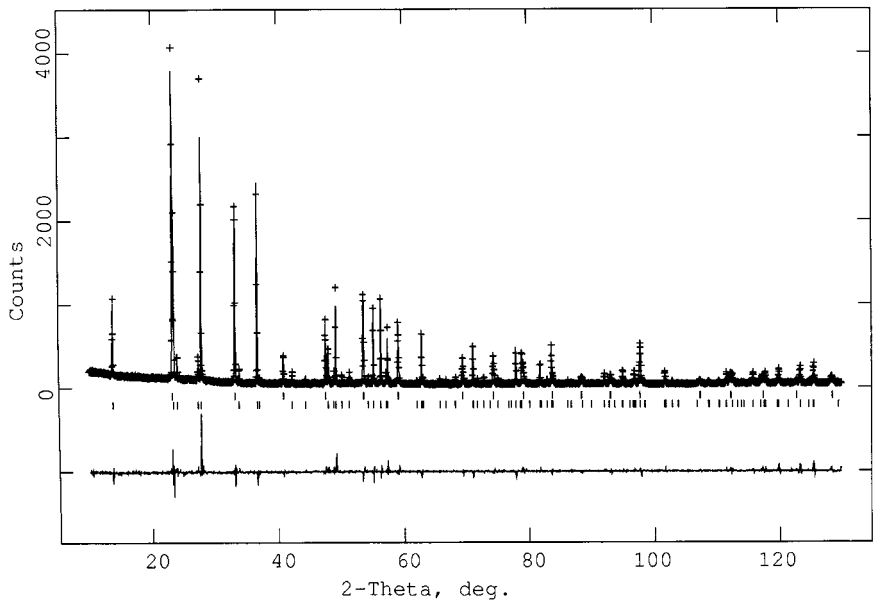

FIG. 2. X-ray Rietveld refinement of $La_{0.108}WO_{3+y}$ (HTB related) + $La_{0.091}WO_3$ (PTB-type) structures. The upper curve illustrates the observed data and the lower is the difference between observed and calculated data. The positions of all allowed Bragg reflections are indicated by the rows of vertical tick marks: PTB (upper) and HTB (lower).

THERMAL STABILITY STUDIES AND PHASE TRANSFORMATION

The DTA curve of the sample *hp*1 in Fig. 3 displays a weak, broad exothermic peak with a maximum at approximately 730°C. Parts of the X-ray powder patterns taken from the starting material and from the final product after the TG treatment are illustrated in Fig. 4. The X-ray pattern in Fig. 4a exhibits strong peaks characteristic of both HTB and PTB phases, whereas the pattern in Fig. 4b only shows strong peaks of the latter compound. This demonstrates that the HTB phase formed under *hp* conditions is transformed to a PTB phase of cubic symmetry when heated in an inert atmosphere under *ap* conditions. The tiny additional peaks in the X-ray pattern (Fig. 4b) could be assigned to a small amount of WO_3 in the sample. The results, summarized in Table 4, show that the volume of the

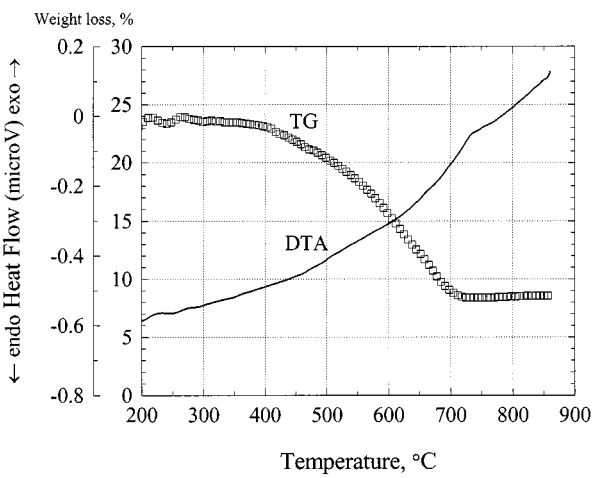

FIG. 3. TG and DTA curves of the bulk sample *hp*1 heated in argon at a rate of 10°C min^{-1}. The TG curve shows a weight loss of ≈ 0.5 wt%. The DTA curve exhibits a weak, broad exothermic peak with a maximum at ≈ 730°C.

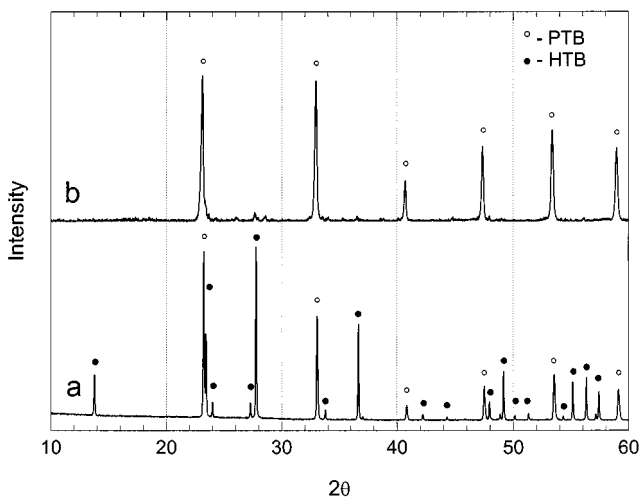

FIG. 4. (a) Part of the X-ray powder pattern of bulk sample *hp*1 before TG/DTA treatment. Peaks characteristic of both HTB (black dots) and PTB (circles) are marked. (b) Part of the X-ray powder pattern of the product after TG/DTA treatment. Only peaks characteristic of PTB can be seen.

cubic unit cell increases slightly during the heat treatment of the *hp* sample. The weak exothermic effect seen in the DTA curve probably reflects the irreversible phase transition *hp*-$La_{0.1}WO_3$ (HTB type) → *ap*-$La_{0.1}WO_3$ (PTB type).

The TG curve in Fig. 3 shows a weight loss of ≈ 0.5 wt% in the temperature region 400 to 700°C during the heating of the sample *hp*1 in an argon atmosphere under *ap* conditions. This weight loss cannot be explained by desorption of gases or release of moisture due to adsorbed water. It seems most likely that it is related to the phase transition above. To study this phenomenon further, the TG experiment in an argon atmosphere was repeated using two additional $La_{0.10}WO_3$ samples, one prepared under *ap* conditions and the other *hp*3 under *hp* conditions at 80 kbar. The TG curves displayed in Fig. 5 clearly show that there is no change in weight of the *ap* sample during the thermal treatment and that the weight loss of the *hp* samples increases with an increasing amount of the HTB related phase in the starting material. This is interpreted in terms of the presence of additional oxygen ions in this phase, most likely located within the six-sided tunnels of the HTB framework structure, thus forming an almost fully oxidized product of composition $La_{0.10}WO_{3+y}$ with $y \approx 0.15$. A change in composition according to the reaction equation

$$La_{0.10}WO_{3.15} \rightarrow La_{0.10}WO_3 + 0.075O_2(g)$$

involves a release of a small amount of oxygen, i.e., a sample weight decrease of ≈ 1 wt%, which is in good agreement with the TG result; see Fig. 5. It also fits with the weight decrease of ≈ 0.5 wt% observed for the sample *hp*1 consisting of ≈ 50 wt% HTB related phase.

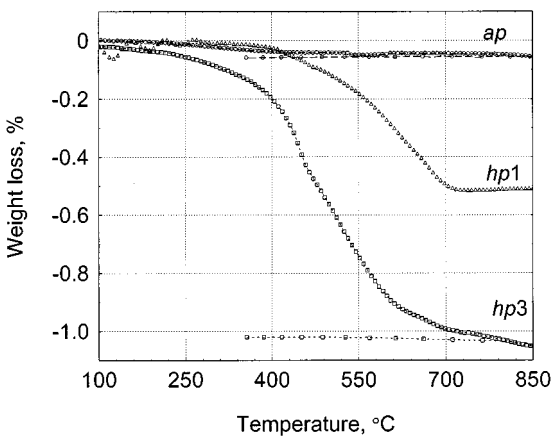

FIG. 5. TG curves of $La_{0.10}WO_3$ samples heated in argon at a rate of 10°C min^{-1}. The samples were prepared at ambient pressure (*ap*) and at 25 kbar (*hp*1) and 80 kbar (*hp*3). They contain 0, ≈ 50, and ≈ 90 wt% of the HTB related phase, respectively.

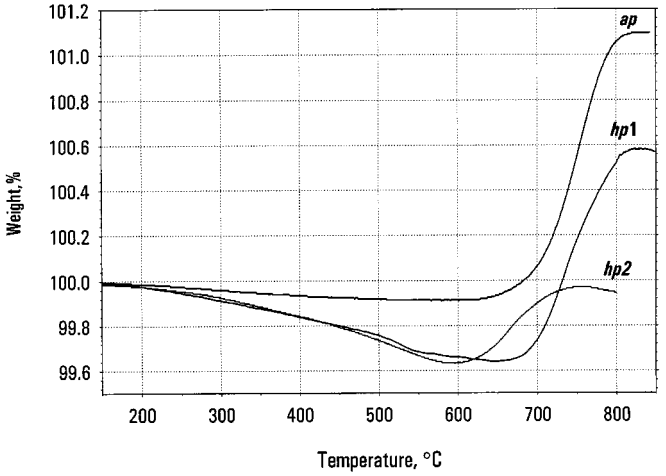

FIG. 6. TG curves of $La_{0.10}WO_3$ samples heated in oxygen at a rate of 3°C min^{-1}. The samples were prepared at ambient pressure (*ap*) and at 25 kbar (*hp*1) and 50 kbar (*hp*2). They contain 0, ≈ 50, and ≈ 90 wt% of the HTB related phase, respectively.

On the other hand, the reverse reaction, oxidation of a $La_{0.10}WO_3$ bronze, would involve a weight increase on the order of ≈ 1 wt%. The oxidation process was studied for three samples of starting composition $La_{0.10}WO_3$, prepared under different experimental conditions. The results presented in Fig. 6 show that oxidation of the PTB compound (*ap* sample) led to an increase in weight of ≈ 1 wt%, whereas oxidation of the sample *hp*2 consisting of ≈ 90 wt% HTB and ≈ 10 wt% WO_3 showed no increase in weight. Oxidation of the sample *hp*1, used in the structure determination, resulted in an increase in weight of ≈ 0.5 wt%, which fits well with the X-ray data above and confirms the ratio HTB : PTB of ≈ 1 : 1. The X-ray powder patterns taken of the three oxidized products were similar and could be interpreted as phase mixtures of $La_{10}W_{22}O_{81}$ (22) and WO_3.

The thermal analysis studies in argon and oxygen atmospheres thus revealed that the HTB related phase is a fully oxidized material of composition La_xWO_{3+y} with $x \approx 0.10$ and $y \approx 3x/2$. The color of the examined samples *hp*1–*hp*3 was a dark blue, however, typical of tungsten bronzes and slightly reduced tungsten oxides, i.e., compounds with tungsten in a valence state somewhat less than + 6. The *y* value in the formula $La_{0.10}WO_{3+y}$ might be slightly less than 0.15. The additional oxygen atoms are most likely located in the six-sided tunnels, thus giving the lanthanum atom a more reasonable coordination number (eight-coordination of oxygen atoms). It is interesting to note that metastable phases of the general formula $M_xWO_{3+x/2}$ with hexagonal tungsten bronze related structures having extra oxygen ions have been synthesized by low-temperature methods for the monovalent cations Li, Na, and K (24, 25).

STRUCTURE REFINEMENT

After refinement of the basic HTB structure of $La_{0.108}WO_3$, an attempt was made to refine the parameters of the additional oxygen atom in the hexagonal tunnel. From the X-ray powder data it was clear that not all the positional and thermal parameters and the occupancy factor of the additional oxygen atom could be refined. The oxygen atom was thus placed at the position $(0, 0, \frac{1}{2})$, and attempts were made to refine the thermal parameter and the occupancy factor. However, it was impossible to refine both these parameters simultaneously due to strong correlation. On the other hand, the X-ray powder pattern and the TG experiments with the *hp*1 sample indicated that approximately 50 wt% of the material was an almost fully oxidized HTB related compound. From these results the y value in the formula $La_{0.108}WO_{3+y}$ could be assumed to be 0.162. This y value corresponds to an occupancy of 0.486 of the onefold (1b) position $(0, 0, \frac{1}{2})$. This value was held fixed in the final Rietveld refinement, which converged and resulted in $R_F = 0.0612$. It should be noted that a rather high U_{iso} value was obtained for the oxygen atom in the six-sided tunnels, probably indicating high mobility of these atoms. The data from the final Rietveld refinement are given within brackets in Table 1.

ELECTRON MICROSCOPY STUDIES

The $La_{0.1}WO_3$ sample *hp*1 was examined in the SEM and TEM microscopes both before and after the thermal analysis study. The shape and the size of the crystals varied considerably in both samples, and there were no discernible differences in habit before and after the thermal treatment. EDS analyses of 16 crystals from the bulk sample in the SEM microscope showed that the average La content was $x = 0.10 \pm 0.01$ and thus in good agreement with that of the starting material. Similar results were obtained with 19 crystals from the same bulk sample after the DTA treatment. Here, the average La content was found to be $x = 0.09 \pm 0.01$. The combined ED and EDS studies of thin crystal fragments from the *hp*1 sample in the TEM microscope confirmed that tungsten bronzes of HTB and PTB structure types were the dominating phases in the bulk product. The ED patterns taken from the HTB crystallites in [001] and [100] orientations (Fig. 7) did not show any streaking of the reflections or any additional superstructure spots. The microanalysis results from the ED–EDS study, given in Table 4, showed that the La content in the HTB-type crystals was in the range $x \approx 0.08$–0.10, thus in rather good agreement with the bulk composition ($x \approx 0.10$) and close to that estimated from the X-ray structure refinement ($x \approx 0.108$). According to the EDS results (TEM), approximately one-third of the hexagonal tunnel sites were filled with randomly distributed La atoms.

The ED patterns taken of the PTB crystals in [100] projection exhibited only the characteristic pattern of intense spots in a square arrangement typical of an ReO_3-type crystal with a cubic cell edge of 3.8 Å. In a few ED patterns taken along [110], weak streaking of the basic reflections and a few weak diffuse superstructure spots could be seen. The composition of most of the PTB crystals, La_xWO_3, was in the range $0.09 \leq x \leq 0.12$, which means that the La contents of the HTB- and PTB-type crystals are approximately equal and in agreement with that of the starting material. A couple of PTB crystals with $x \approx 0.2$ were observed, and the ED patterns of these exhibited streaking and superstructure reflections, as demonstrated in Fig. 8. Similar observations have been made recently on PTB crystals from bulk samples of composition RE_xWO_3 with $x = 0.1$–0.3 and RE = La or Nd, prepared by conventional

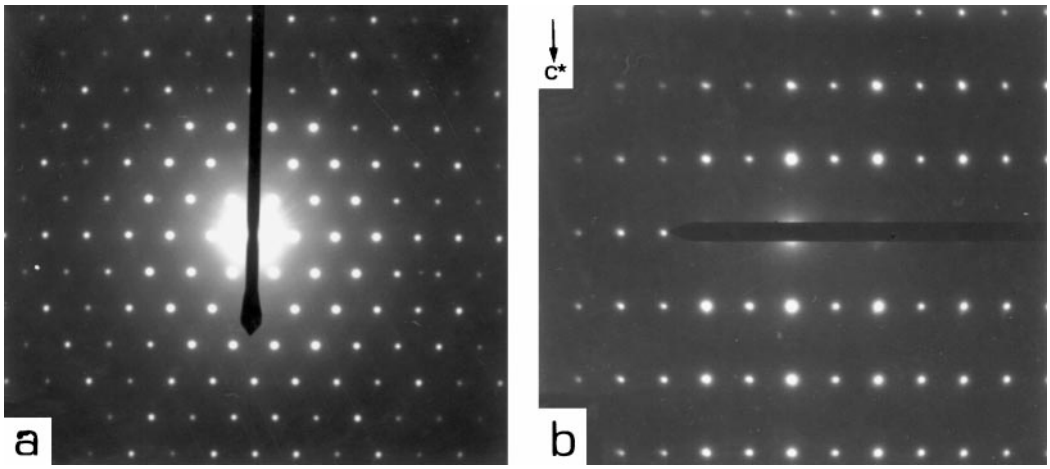

FIG. 7. ED patterns of a HTB-type crystal in (a) [001] and (b) [100] projections.

TABLE 4
Sample Compositions, Experimental Conditions, Phase Identification from X-ray Powder and ED Patterns, Cell Parameters Refined from the X-ray Data, and ED–EDS Results (TEM)

Starting composition	Experimental conditions	Phase	Unit cell dimensions			ED–EDS results
			a (Å)	c (Å)	V (Å^3)	x
$La_{0.1}WO_3$	$T = 1250°C$	HTB	7.40890(5)	3.79239(4)	180.28	0.08–0.10
(*hp*1)	$P = 25$ kbar	PTB	3.82458(6)		55.94	0.09–0.12, ≈ 0.20
$La_{0.1}WO_3$	After DTA up to	PTB	3.8391(9)		56.58	0.10–0.14
(*hp*1)	$T = 850°C$	WO_3				
$La_{0.1}WO_3$	$T = 1200°C$	HTB	7.4070(5)	3.7936(3)	180.25	0.08–0.13
(*hp*2)	$P = 50$ kbar	WO_3				
$La_{0.1}WO_3$	$T = 1200°C$	HTB	7.4037(4)	3.7951(3)	180.15	0.07–0.10
(*hp*3)	$P = 80$ kbar	W_3O_8(II)				
$La_{0.1}WO_3$	After DTA up to	PTB	3.8265(2)		56.03	0.10–0.14
(*hp*3)	$T = 850°C$	WO_3				
$La_{0.1}WO_3$	$T = 900°C$	PTB	3.840		56.60	0.11–0.13
(*ap*)	evacuated Si tube					

solid-state synthesis (26). High-resolution transmission electron microscopy (HRTEM) images of the latter crystals have revealed some local ordering of the *RE* atoms in the structure and this may be the origin also in the present case. In addition to the *hp*-$La_{\approx 0.1}WO_{3+y}$ compounds with HTB and PTB related structures, the EDS data revealed a couple of tungsten oxide fragments, $WO_{\approx 3}$, and one crystallite with an La : W ratio of 50 : 50 at.%. The unit cell dimensions of the latter phase are still unknown. The X-ray and ED–EDS data on the main phases in the *hp*1–*hp*3 samples are summarized in Table 4.

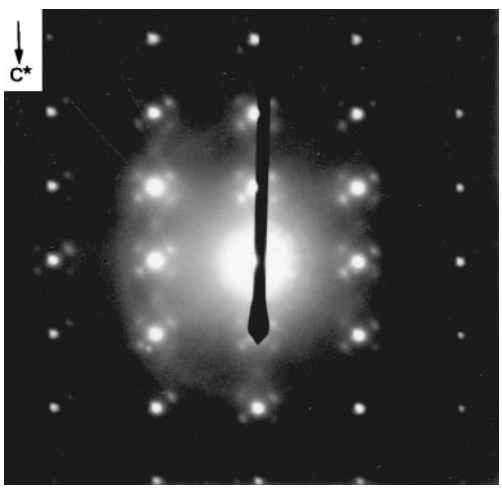

FIG. 8. ED pattern of a PTB-type crystal aligned with the [110] direction of the cubic PTB cell parallel to the electron beam. Streaking of the basic reflections and diffuse superstructure spots can be seen.

From the X-ray and ED–EDS results it was obvious that PTB-type crystals dominated in the *hp*1 sample after the thermal treatment. The ED patterns were very similar to those taken of PTB-type crystals before the DTA treatment. Streaking and superstructure reflections similar to those in Fig. 8 were sometimes observed. The average La content in the crystals was $x \approx 0.12$ (Table 4), which is only slightly higher than that of the starting material ($x = 0.10$). The ED–EDS study also showed that a small amount of WO_3 crystals was present in the sample. It is noteworthy that no ED pattern characteristic of an HTB-type crystal or showing an intergrowth of HTB- and a ReO_3-type structure has been seen in these samples. The electron microscopy results thus support the conclusion that the *hp*-$La_{0.1}WO_{3+y}$ compound with an HTB related structure transforms into a PTB-type structure of composition $La_{\approx 0.1}WO_3$ during the thermal analysis treatment in argon under ambient pressure conditions.

The electron microscopy investigations of the other two *hp* samples, *hp*2 and *hp*3, confirmed the X-ray results presented above. ED patterns characteristic of HTB-type crystals were frequently obtained from thin crystallites of the samples before the thermal treatment. The average La content in these crystals was in the range $x = 0.07$–0.13 (see Table 4). The ED–EDS studies also showed that some crystals of WO_3 were present in the *hp*2 sample, whereas ED patterns characteristic of W_3O_8(II) crystals were obtained from the *hp*3 sample. It is noteworthy that no PTB-type crystals were seen in the samples before the TG-DTA studies. On the other hand, ED–EDS studies of thin crystallites from the *hp*3 sample after the DTA treatment revealed only

WO_3 and PTB-type crystals. The average La content in the latter crystals was slightly larger ($x \approx 0.12$) than that ($x \approx 0.09$) observed in the HTB related crystals before the thermal treatment in argon. The reason for this might be that the *hp*-HTB related phase prefers filling the six-sided tunnels, which is slightly less than one-third, whereas the PTB-type structure can easily accommodate a somewhat higher La content.

DESCRIPTION OF THE STRUCTURE AND DISCUSSION

From the X-ray powder patterns and from the electron microscopy results it is not possible to determine if the HTB related phase formed under *hp* conditions is a hexagonal tungsten bronze of composition $La_{0.10}WO_3$ or a lanthanum tungstate of composition $La_{0.10}WO_{3.15}$. However, from the X-ray powder data and from the ED patterns it is clear that the *hp* compound has a basic framework structure of HTB type, which is similar to those previously reported for Sn_xWO_3 ($x = 0.26$–0.33) (16) and $Ge_{0.24}WO_3$ (8). The W–O and *M*–O bond distances in the framework structure of WO_3(hex) (11) and $La_{0.108}WO_{3.162}$ (HTB type) and in the related Sn- and Ge-containing phases are given in Table 5. In the present study it has not been possible to refine the coordinates of the O2 position, so the interatomic distances might have large standard errors. The M_xWO_3 (M = La, Sn, and Ge) compounds all have a short crystal *c* axis of ≈ 3.8 Å, and the W atoms are located in the *xy* plane at $z = 0$. The W–O distances are in the range 1.88–1.95 Å, and the mean W–O values are fairly similar. The HTB framework structure, consisting of slightly distorted WO_6 octahedra linked by corners (Fig. 1) thus seems to be approximately the same in these bronzes. The main differences between the compounds are the location of the *M* atoms in the six-sided tunnels and the occupancy of the *M* atom sites. The Rietveld results above indicate that the lanthanum atoms in the $La_{0.10}WO_3$ structure are located on the hexagonal axis, not in the *xy* plane at $z = 0$ but randomly distributed on two positions approximately 0.18 Å distant from that plane. The latter sites give rise to six La–O distances of equal length (2.695 Å), which are only slightly longer than those (2.684 Å) generated from an atom located at the (0, 0, 0) position, but shorter than the 12 La–O distances, calculated to be 2.7044 Å, in the PTB structure of $La_{0.091}WO_3$ in Table 1. In the Sn–HTB and Ge–HTB structures, the *M* atoms are located in the *xy* plane at $z = 0$, but displaced from the tunnel center. The resulting six *M*–O distances are all in the range 2.2–3.8 Å (Table 5). The cation radius of La^{3+} ($r_{La3+} = 1.032$ Å (27)) is larger than those of Ge^{2+} ($r_{Ge2+} = 0.73$ Å (27)) and Sn^{2+} ($r_{Sn2+} \approx 0.9$ Å (16)). The latter two cations also have lone-pair electrons (s^2) that should play an important role in the location of these ions in the tunnels. These facts support our X-ray results that the La^{3+} cations are located on the central hexagonal tunnel axis. In the alkali tungsten bronzes, A_xWO_3, of HTB type, the alkali ions ($A = K^+$, Rb^+, and Cs^+) are located at 12-coordinated sites in the hexagonal tunnels between the tungsten layers ($z = \frac{1}{2}$). As La^{3+} is much smaller than the alkali ions, it seems reasonable that La^{3+} is located at a different position on the hexagonal axis. The thermal analysis results from the *hp* samples indicate that there are extra oxygen atoms (at $y \approx 0.15$) in the HTB structure. The results from the Rietveld refinement described above weakly support the idea that these atoms reside in the six-sided tunnels. The additional oxygen ions will compensate for the high charge (3 +) of lanthanum in the tunnels and give eight-coordinated lanthanum atoms. More information about the oxygen-atom arrangement might be obtained from neutron diffraction data. However, at the present stage it seems impossible to prepare single-phase *hp*-$La_{0.10}WO_{3.15}$ in sufficient quantity for neutron diffraction experiments.

It has not been possible to prepare La_xWO_3 of HTB-structure type by conventional solid-state synthesis under high-temperature and ambient-pressure conditions. The use of high pressure during synthesis appears thus to be crucial for the formation of the HTB related phase. The $RE_{0.10}WO_{3+y}$ phase of the HTB related structure is

TABLE 5
Unit Cell, Space Group, and Bond Distances of HTB-Type Structures

Compound	WO_3 (hex)	La–HTB	Sn–HTB	Ge–HTB
a axis	7.2982 Å	7.4089 Å	7.429 Å	7.440 Å
c axis	3.899 Å[a]	3.7924 Å	3.7868 Å	3.817 Å
Space group	*P6/mmm*	*P6/mmm*	*P6/mmm*	*P622*
W–O1	1.9495 Å	1.8962 Å	1.8934 Å	1.9085 Å
W–O1	1.9495 Å	1.8962 Å	1.8934 Å	1.9085 Å
W–O2	1.8867 Å	1.9291 Å	1.9154 Å	1.9244 Å
W–O2	1.8867 Å	1.9291 Å	1.9154 Å	1.9244 Å
W–O2	1.8867 Å	1.9291 Å	1.9412 Å	1.9244 Å
W–O2	1.8867 Å	1.9291 Å	1.9412 Å	1.9244 Å
Average W–O dist.	1.9076 Å	1.9181 Å	1.9167 Å	1.9191 Å
M–O2		2.6954 Å	2.2163 Å	2.2532 Å
M–O2		2.6954 Å	2.3916 Å	2.2532 Å
M–O2		2.6954 Å	2.6641 Å	2.7868 Å
M–O2		2.6954 Å	2.7902 Å	2.7868 Å
M–O2		2.6954 Å	3.0329 Å	3.2335 Å
M–O2		2.6954 Å	3.0886 Å	3.2335 Å
Average *M*–O dist		2.6954 Å	2.6973 Å	2.7578 Å
References	(11)	This study	(16)	(8)

[a] Average structure given, true cell parameter $a = 7.298(2)$ Å and $c = 7.798(3)$ Å and probable space group $P6_3/mcm$.

metastable and decomposes during heating under ambient-pressure conditions to a two-phase mixture of a thermodynamically stable RE_xWO_3 ($x \approx 0.1$) bronze of cubic PTB-type structure and a small amount of WO_3. The phase transformation mechanism seems to differ, however, from the nucleation-and-growth mechanism previously reported for the WO_3(hex) $\rightarrow$ WO_3(mon) transition (28) since no electron diffraction pattern or HRTEM image of coexisting *RE*–HTB and *RE*–PTB phases has yet been observed. The *RE* and O atoms in the hexagonal tunnels seem to stabilize the HTB framework, for the phase transition (*RE*–HTB $\rightarrow$ *RE*–PTB) takes place at a higher temperature (600–700°C) than that (400°C) observed for WO_3(hex) $\rightarrow$ WO_3(mon).

ACKNOWLEDGMENTS

The authors wish to thank Professor P.-E. Werner for valuable discussions and comments on the X-ray structure determination. The research described here was partly made possible by a Visiting Scientist Grant from the Royal Swedish Academy of Sciences through its Nobel Institute for Chemistry. This support is gratefully acknowledged. The present study forms a part of a research project financially supported by the Swedish Natural Science Research Council and the Russian Foundation for Basic Research (Grant 01-03-32457).

REFERENCES

1. N. D. Zakharov, P.-E. Werner, Z. Liliental–Weber, V. P. Filonenko, I. P. Zibrov, and M. Sundberg, *Mater. Res. Bull.* **31,** 373 (1996).
2. C. Grenthe, M. Sundberg, V. P. Filonenko, and I. P. Zibrov, *J. Solid State Chem.* **154,** 466 (2000).
3. W. Ostertag, *Inorg. Chem.* **5,** 758 (1966).
4. P. J. Wiseman and P. G. Dickens, *J. Solid State Chem.* **17,** 91 (1976).
5. A. Magnéli, *Acta Chem. Scand.* **7,** 313 (1953).
6. A. Hussain, *Chem. Commun. Univ. Stockholm.* **No 2** (1978).
7. Ph. Labbe, M. Goreaud, B. Raveau, and J. C. Monier, *Acta Crystallogr. B* **34,** 1433 (1978).
8. V. Plies, *Z. Anorg. Allg. Chem.* **521,** 191 (1985).
9. L. Kihlborg and A. Hussain, *Mater. Res. Bull.* **14,** 667 (1979).
10. Ph. Labbe, M. Goreaud, B. Raveau, and J. C. Monier, *Acta Crystallogr. B* **35,** 1557 (1979).
11. B. Gerand, G. Nowogrocki, J. Guenot, and M. Figlarz, *J. Solid State Chem.* **29,** 429 (1979).
12. M. Figlarz, B. Gerand, B. Dumont, A. Delahaye-Vidal, and F. Portemer, *Phase Transitions* **31,** 167 (1991).
13. K. H. Cheng, A. J. Jacobson, and M. S. Whittingham, *Solid State Ionics.* **5,** 355 (1981).
14. R. C. T. Slade, B. C. West, and G. P. Hall, *Solid State Ionics* **32/33,** 154 (1989).
15. A. Martínez de la Cruz, L. M. Torres-Martínez, F. Garcia-Alvarado, E. Moran, and M. A. Alario-Franco, *Solid State Ionics* **84,** 181 (1996).
16. X.-L. Xu, H. W.Schmalle, and J. R. Günter, *Solid State Ionics* **76,** 221 (1995).
17. I. P. Zibrov, V. P. Filonenko, P.-E. Werner, B.-O. Marinder, and M. Sundberg, *J. Solid State Chem.* **141,** 205 (1998).
18. K.-E. Johansson, T. Palm, and P.-E. Werner, *J. Phys E* **13,** 1289 (1980).
19. P.-E. Werner, *Arkiv. Kemi.* **31,** 513 (1969).
20. M. Sundberg, N. D. Zakharov, I. P. Zibrov, Yu. A. Barabanenkov, V. P. Filonenko, and P.-E. Werner, *Acta Crystallogr. B* **49,** 951 (1993).
21. A. C. Larson and R. B. Von Dreele, Los Alamos National Laboratory, Report N LA-UR-86-748, 1987.
22. M. Yoshimura, H. Morikawa, and M. Miyaki, *Mater. Res. Bull.* **10,** 1221 (1975).
23. R. J. Hill and H. D. Flack, *J. Appl. Cryst.* **20,** 356 (1987).
24. K. P. Reis, A. Ramanan, and M. S. Whittingham, *J. Solid State Chem.* **96,** 31 (1992).
25. L. Hernán, M. Macias, J. Morales, L. Sánchez, and J. L. Tirado, *Solid State Ionics* **47,** 75 (1991).
26. C. Grenthe and M. Sundberg, in preparation.
27. R. D. Shannon, *Acta Crystallogr. A* **32,** 751 (1976).
28. M. Figlarz, B. Dumont, B. Gerand, and B. J. Beaudoin, *Microsc. Spectrosc. Electron.* **7,** 371 (1982).